

Symbol Detection for Coarsely Quantized OTFS

Junwei He, Haochuan Zhang*, Chao Dong, and Huimin Zhu

Abstract—This paper explicitly models a coarse and noisy quantization in a communication system empowered by orthogonal time frequency space (OTFS) for cost and power efficiency. We first point out, with coarse quantization, the effective channel is imbalanced and thus no longer able to circularly shift the transmitted symbols along the delay-Doppler domain. Meanwhile, the effective channel is non-isotropic, which imposes a significant loss to symbol detection algorithms like the original approximate message passing (AMP). Although the algorithm of generalized expectation consistent for signal recovery (GEC-SR) can mitigate this loss, the complexity in computation is prohibitively high, mainly due to an dramatic increase in the matrix size of OTFS. In this context, we propose a low-complexity algorithm that incorporates into the GEC-SR a quick inversion of quasi-banded matrices, reducing the complexity from a cubic order to a linear order while keeping the performance at the same level.

Index Terms—OTFS, coarse quantization, GEC-SR, matrix inversion, low-complexity.

I. INTRODUCTION

Interest in estimating signal parameters from quantized data has been increased significantly in recent years [1]. Ultra-wideband applications, such as millimeter-wave communications, require high sampling rates, but conventional analog-to-digital converters (ADCs) are expensive and power-hungry. In cases that are cost and power constrained, the use of high-precision ADCs is not feasible, which makes ADCs with coarse quantization a better choice for systems like 6G [2].

For 6G a prominent waveform candidate is *orthogonal time frequency space (OTFS)* [3, 4], a 2D modulation technique that transforms the information to the delay-Doppler (DD) coordinate. OTFS enjoys an excellent robustness in high-speed vehicular scenarios, while orthogonal frequency division multiplexing (OFDM) suffers from disrupted orthogonality among subcarriers due to the high Doppler shift.

Detection for symbols in the delay-Doppler domain is key to the OTFS communications. Linear detectors like LMMSE are usually prior-ignorant, i.e., they are unaware of the prior information of transmitted symbols, and therefore not optimal in general sense. Non-linear detectors like sphere decoding are optimal in detection accuracy but often suffer from an unaffordable computational complexity. An effective and efficient alternative is to use message passing algorithm for the detection of OTFS symbols. A great number of prior works has already been dedicated to this topic: [5] designed a hybrid

detection algorithm that combines MAP and parallel interference cancellation; [6] detected the signals in both time and DD domains iteratively using a unitary transformation; [7] developed a message passing algorithm that utilized the sparsity of the effective channel; [8] applied expectation propagation (EP) to the detection and reduced significantly its complexity by exploiting the channel structure; [9] proposed an unitary approximate message passing (UAMP) based new algorithm, addressing the challenge of large channel paths and fractional Doppler shifts, effectively and efficiently; [10] circumvented the matrix inversion of vector approximate message passing (VAMP) by an average approximation. These works, however, considered only the ideal case of infinite-precision ADCs. The influence of coarse quantization is not yet accounted for.

This paper models explicitly the coarse and noisy quantization for the OTFS communications. We find that a major difference between coarse quantization and the infinite-precision case is: the effective channel is no longer a multiplication of three matrices, i.e., the postprocessing transform, the multipath fast-fading channel, and the preprocessing transform; instead, a non-linear mapping enters between the postprocessing and the remaining two, making it impossible to model them as an integrated whole. Ignoring the difference and applying directly the algorithms above is seen to bring about noticeable performance loss. To overcome the limitation, we consider a generalized linear model (GLM) [11] that takes in the noisy quantization, the fast-fading channel, and the preprocessing transform, and validate the performance of two efficient solvers, GAMP [11] and GEC-SR [12]. We find that GEC-SR is much robust to the change of effective channel; however, the complexity of GEC-SR quickly soars up as the matrix size in OTFS squares that of the OFDM counterpart.

In this context, we propose a low-complexity GEC-SR, which utilizes a quick inversion of the quasi-banded matrices. The idea of inverting a quasi-banded matrix was not new [8, 13]; however, the channel matrix here is asymmetric (due to a lack of the postprocessing transform), and the matrix to invert is in general not quasi-banded. Interestingly, we find that if we approximate the GEC-SR covariance matrix by a scaled identity matrix, the one to invert simply reduces to be quasi-banded. It is also worth noting the method of [8] is not applicable to coarse quantization, because [8, Eq. (40)] holds only in the quantization-free case. Finally, we carry out simulations to confirm the effectiveness of the proposed algorithm.

Summing up, the contributions of this paper are two-folded:

- We point out, in the presence of coarse quantization, the effective channel becomes imbalanced, containing only one of two transform matrices, which makes the OTFS modulation unable to circularly shift the transmitted symbols along the delay-Doppler domain as designed.

J. He and H. Zhang are with Guangdong University of Technology, Guangzhou, China (e-mails: sikouhju@gmail.com; haochuan.zhang@gdut.edu.cn). C. Dong is with Beijing University of Posts and Telecommunications, Beijing, China (e-mail: dongchao@bupt.edu.cn). H. Zhu is with Guangzhou University of Chinese Medicine, Guangzhou, China (e-mail: hm_zhu@gzucm.edu.cn). This work was supported by Guangdong Basic and Applied Basic Research Foundation under Grant 2022A1515010196. *Corresponding author: H. Zhang.

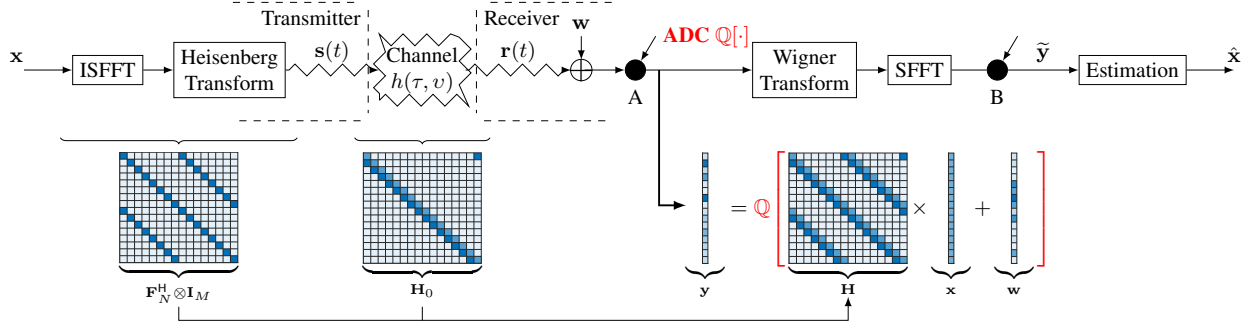


Fig. 1. An example on communication via OTFS with finite-precision ADC at the receiver, where $M = 8$, $N = 2$, $P = 2$, $k_{\max} = 8$ and $l_{\max} = 2$.

- We propose a low-complexity algorithm for detecting data symbols in an OTFS system coarsely quantized, which incorporates a quick inversion of the quasi-banded matrices into GEC-SR, thus reducing the complexity from cubic order to linear order while maintaining the detection accuracy at a negligible level.

II. SYSTEM MODEL FOR OTFS COARSELY QUANTIZED

Fig. 1 presents a block diagram of the (coarsely) quantized OTFS communication system, where $\mathbb{Q}[\cdot]$ is the ADC quantization located at Position A of Fig. 1, whose mathematical description is left to the appendix. Here, the received signal is

$$\tilde{\mathbf{y}} = (\mathbf{F}_N \otimes \mathbf{I}_M) \underbrace{\mathbb{Q}[\mathbf{H}_0 (\mathbf{F}_N^H \otimes \mathbf{I}_M) \mathbf{x} + \mathbf{w}]}_{\mathbf{H}}, \quad (1)$$

where $\mathbf{x} = \text{vec}(\mathbf{X})$ and $\tilde{\mathbf{y}} = \text{vec}(\tilde{\mathbf{Y}})$, with $\mathbf{X} \in \mathbb{C}^{M \times N}$ and $\tilde{\mathbf{Y}} \in \mathbb{C}^{M \times N}$ being the data symbols in the delay-and-Doppler domain at the transmitter and receiver, respectively, while $\text{vec}(\cdot)$ is the vectorization of a matrix. The matrix $\mathbf{H}_0 \in \mathbb{C}^{MN \times MN}$ is the multi-path fast-fading channel. The vector \mathbf{w} is an additive white Gaussian noise (AWGN), with σ^2 being its variance. The matrix \mathbf{F}_M is the normalized M -point discrete Fourier transform matrix, whose (m, n) -th element is defined as $\mathbf{F}_M(m, n) = \frac{1}{\sqrt{M}} e^{-j \frac{2\pi m n}{M}}$, and \mathbf{I}_M is an identity matrix. The numbers of subcarriers and time slots in the OTFS modulation are M and N , respectively, while $(\cdot)^H$ is the conjugate transpose, and \otimes is the Kronecker product. \mathbf{H}_0 is modeled as [8, 9, 14]: $\mathbf{H}_0 = \sum_{i=1}^P h_i \Pi^{l_i} \Delta^{k_i}$, where $\Pi = \begin{bmatrix} 0 & \dots & 0 & 1 \\ 1 & \dots & 0 & 0 \\ \vdots & \ddots & \vdots & \vdots \\ 0 & \dots & 1 & 0 \end{bmatrix}$ is an $MN \times MN$ permutation matrix, and Δ is an $MN \times MN$ diagonal matrix with non-zero elements $\{z^0, \dots, z^{MN-1}\}$ with $z = e^{j \frac{2\pi}{MN}}$. The parameter h_i is the i -th channel gain, and P is the number of channel paths.

It is worth noting the coarsely quantized model (1) differs distinctly from the ideal (infinite-precision) case below

$$\mathbf{y}_{\text{ideal}} = \underbrace{(\mathbf{F}_N \otimes \mathbf{I}_M) \mathbf{H}_0 (\mathbf{F}_N^H \otimes \mathbf{I}_M)}_{\mathbf{H}_{\text{ideal}}} \mathbf{x} + \mathbf{w}, \quad (2)$$

where the ideal channel matrix $\mathbf{H}_{\text{ideal}}$ is symmetric, and in effect it cyclically shifts the data symbols \mathbf{X} on a delay-Doppler grid/lattice [15] (recall that $\mathbf{x} = \text{vec}(\mathbf{X})$). In contrast, the introduction of $\mathbb{Q}[\cdot]$ to (1) breaks down the symmetry and brings in an effective channel \mathbf{H} that is imbalanced. Even in

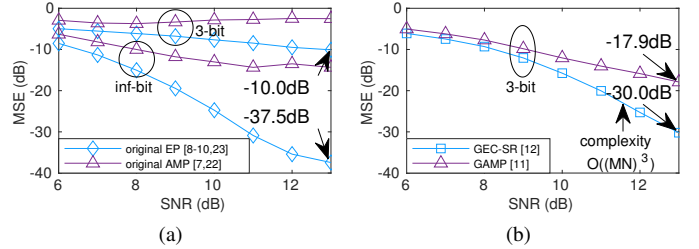


Fig. 2. MSE performance of four algorithms from the AMP and the EP families in $P = 16$ case: (a) The original EP [8–10, 23] outperforms the original AMP [7, 22] in the infinite-precision case; (b) Their generalized versions can handle the coarse quantization effectively, with GEC-SR [12] being the best of the four.

the extreme case of a single path and zero Doppler shift, i.e., $\mathbf{H}_0 = \mathbf{I}_{MN}$, the two matrices are not identical: $\mathbf{H}_{\text{ideal}} \neq \mathbf{H}$; therefore, the quantized effective channel \mathbf{H} is no longer able to circularly shift the transmitted symbols along the delay-Doppler domain. To keep notations uncluttered, we perform prewhitening on $\tilde{\mathbf{y}}$

$$\mathbf{y} = (\mathbf{F}_N \otimes \mathbf{I}_M)^{-1} \tilde{\mathbf{y}} = (\mathbf{F}_N^H \otimes \mathbf{I}_M) \tilde{\mathbf{y}}, \quad (3)$$

and rewrite the signal model (1) in a concise form as

$$\mathbf{y} = \mathbb{Q}[\mathbf{H}\mathbf{x} + \mathbf{w}] = \mathbb{Q}[\mathbf{z} + \mathbf{w}]. \quad (4)$$

Although the system model (4) looks very similar to quantized compressed sensing and quantized massive MIMO in [16–21], the situation here is quite different. Our matrix \mathbf{H} is circulant and thus correlated, but in the prior works it was assumed isotropic, typically i.i.d. Gaussian. Ref. [21] concluded that a correlated matrix \mathbf{H} will degrade the performance of the AMP-like algorithms, and this is connected to the fact that $\mathbf{H}\mathbf{x}$ is no longer i.i.d. Gaussian. We have similar observation here: in the ideal case of Fig. 2a, the original AMP [7, 22] is seen to suffer from a severe performance loss, while its EP counterpart [8–10, 23] performs much better, as it treats each row of the matrix as one unit. However, the original EP is also not as effective in the case of coarse quantization: changing the precision from infinite- to 3-bit will impose a 27.5 dB loss in MSE, as evidenced by Fig. 2a. To combat coarse quantization, we apply GEC-SR algorithm [12], an enhancement to the original EP, and find it rather robust to the change of precision, outperforming GAMP [11] noticeably, see Fig. 2b.

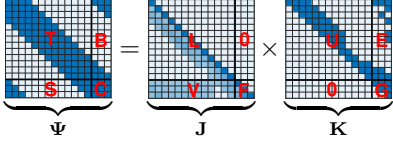


Fig. 3. An example on the LU decomposition of a quasi-banded matrix Ψ , where $M = 8$, $N = 2$, $P = 6$, $k_{\max} = 8$, and $l_{\max} = 3$.

III. THE PROPOSED ALGORITHM

Despite its robustness, the iterative algorithm GEC-SR [12] suffers from a high computational complexity, which is on the order of $\mathcal{O}(T(MN)^3)$, where T is the number of iterations. The complexity is primarily centered on the matrix inversion

$$[\mathbf{H}^H \text{Diag}(\mathbf{1} \odot \mathbf{v}_1^-) \mathbf{H} + \text{Diag}(\mathbf{1} \odot \mathbf{v}_0^+)]^{-1}, \quad (5)$$

where \mathbf{v}_1^- and \mathbf{v}_0^+ are parameters related to the variances, \odot is component-wise division, and $\text{Diag}(\mathbf{d})$ is a diagonal matrix with non-zero elements \mathbf{d} . One way to ease the burden of computation is to approximate the diagonal matrices by scaled identity ones and then perform an SVD on \mathbf{H} before the iteration. In other words, we approximate (5) by

$$\left[\frac{\mathbf{H}^H \mathbf{H}}{v_1^-} + \frac{\mathbf{I}}{v_0^+} \right]^{-1} = (\mathbf{F}_N \otimes \mathbf{I}_M) \underbrace{\left[\frac{\mathbf{H}_0^H \mathbf{H}_0}{v_1^-} + \frac{\mathbf{I}}{v_0^+} \right]^{-1}}_{\Psi} (\mathbf{F}_N^H \otimes \mathbf{I}_M) \quad (6)$$

Even in this case, the complexity of $\mathcal{O}((MN)^3)$ [24] is still very high, as the OTFS matrix size has increased from $M \times N$ to $MN \times MN$, where $M \approx 50$ and $N \approx 50$, typically [25].

Fortunately, the matrix Ψ has a particular structure that admits a fast computation for its inverse. To see this, we first note that Ψ is *quasi-banded* [8], as shown in Fig. 3. A fully banded matrix is very effective to invert using its LU decomposition, where the complexity is on the order of $\mathcal{O}(l_{\max}^2 MN)$, with l_{\max} being the maximum delay. So, we further look into the quasi-banded structure of Ψ and see that, although not fully banded, the matrix contains a major part \mathbf{T} that is fully banded and some minor ones \mathbf{B} , \mathbf{S} , and \mathbf{C} without a particular structure. In this context, we denote the LU decomposition of Ψ as [8, 13, 26]:

$$\underbrace{\begin{bmatrix} \mathbf{T}_{Q \times Q} & \mathbf{B}_{Q \times P} \\ \mathbf{S}_{P \times Q} & \mathbf{C}_{P \times P} \end{bmatrix}}_{\Psi} = \underbrace{\begin{bmatrix} \mathbf{L}_{Q \times Q} & \mathbf{0}_{Q \times P} \\ \mathbf{V}_{P \times Q} & \mathbf{F}_{P \times P} \end{bmatrix}}_{\mathbf{J}} \times \underbrace{\begin{bmatrix} \mathbf{U}_{Q \times Q} & \mathbf{E}_{Q \times P} \\ \mathbf{0}_{P \times Q} & \mathbf{G}_{P \times P} \end{bmatrix}}_{\mathbf{K}}$$

where $P = l_{\max}$ and $Q = MN - P$. The matrices \mathbf{L} , \mathbf{V} , \mathbf{F} , \mathbf{U} , \mathbf{E} , and \mathbf{G} can be determined by following four steps:

$$(\mathbf{L}, \mathbf{U}) := \mathbb{LU}[\mathbf{T}] \quad (7a) \quad \mathbf{V} := \mathbf{S}\mathbf{U}^{-1} \quad (7c)$$

$$\mathbf{E} := \mathbf{L}^{-1}\mathbf{B} \quad (7b) \quad (\mathbf{F}, \mathbf{G}) := \mathbb{LU}[\mathbf{C} - \mathbf{VE}] \quad (7d)$$

The overall complexity of these steps is $\mathcal{O}(l_{\max}^2 MN)$:

- 1) \mathbf{T} is banded, and $\mathbb{LU}[\mathbf{T}]$ is $\mathcal{O}(MN)$ [26].
- 2) \mathbf{L} is lower triangular by definition, and \mathbf{L}^{-1} is $\mathcal{O}(l_{\max}^2 MN)$ [8, Algorithm 2], while \mathbf{U} is similar.
- 3) $\mathbf{C} \in \mathbb{C}^{P \times P}$ is small in size ($P \ll MN$), and the complexity of $\mathbb{LU}[\mathbf{C} - \mathbf{VE}]$ is negligible.

Given \mathbf{J} and \mathbf{K} , we invert the two block matrices and obtain

$$\Psi^{-1} = \begin{bmatrix} \mathbf{U}^{-1} & -\mathbf{U}^{-1}\mathbf{E}\mathbf{G}^{-1} \\ \mathbf{0} & \mathbf{G}^{-1} \end{bmatrix} \begin{bmatrix} \mathbf{L}^{-1} & \mathbf{0} \\ -\mathbf{F}^{-1}\mathbf{V}\mathbf{L}^{-1} & \mathbf{F}^{-1} \end{bmatrix}$$

Algorithm 1: The proposed algorithm

Input: $p(\mathbf{y}|\mathbf{z})$, $p(\mathbf{x})$, \mathbf{H} , $\tilde{\mathbf{y}}$
Preprocess: $\mathbf{y} = (\mathbf{F}_N \otimes \mathbf{I}_M)^{-1} \tilde{\mathbf{y}}$
Initialize: $t = 1$, $\mathbf{m}_1^+ = \mathbf{0}$, $v_1^+ = 1$, $\mathbf{m}_0^+ = \mathbf{0}$, $v_0^+ = 1$,
 $\Psi(v_1^-, v_0^+) = [\mathbf{H}^H \mathbf{H} / v_1^- + \mathbf{1} / v_0^+ \mathbf{I}]$
Iterate: while $t \leq T$ do
 $\hat{\mathbf{z}}^- = \mathbb{E}[\mathbf{z}|\mathbf{m}_1^+, v_1^+ \mathbf{1}]$
 $\mathbf{v}_z^- = \text{Var}[\mathbf{z}|\mathbf{m}_1^+, v_1^+ \mathbf{1}]$
 $\bar{v}_z^- = \text{mean}(\mathbf{v}_z^-)$
 $v_1^- = 1 \odot (1 \odot \bar{v}_z^- - 1 \odot v_1^+)$
 $\mathbf{m}_1^- = (v_1^- \mathbf{1}) \odot (\hat{\mathbf{z}}^- \odot (v_1^- \mathbf{1}) - \mathbf{m}_1^+ \odot (v_1^+ \mathbf{1}))$
 $\Psi^{-1} = \text{function_matrix_inverse}[\Psi(v_1^-, v_0^+)]$
 $\mathbf{Q}_x^- = (\mathbf{F}_N \otimes \mathbf{I}_M) \Psi^{-1} (\mathbf{F}_N^H \otimes \mathbf{I}_M)$
 $\mathbf{v}_x^- = \text{diag}(\mathbf{Q}_x^-)$
 $\bar{v}_x^- = \text{mean}(\mathbf{v}_x^-)$
 $\hat{\mathbf{x}}^- = \mathbf{Q}_x^- (\mathbf{H}^H \text{Diag}(\mathbf{1} \odot (v_1^- \mathbf{1})) \mathbf{m}_1^- + \mathbf{m}_0^+ \odot (v_0^+ \mathbf{1}))$
 $v_0^- = 1 \odot (1 \odot \bar{v}_x^- - 1 \odot v_0^+)$
 $\mathbf{m}_0^- = (v_0^- \mathbf{1}) \odot (\hat{\mathbf{x}}^- \odot (v_0^- \mathbf{1}) - \mathbf{m}_0^+ \odot (v_0^+ \mathbf{1}))$
 $\hat{\mathbf{x}}^+ = \mathbb{E}[\mathbf{x}|\mathbf{m}_0^-, v_0^- \mathbf{1}]$
 $\mathbf{v}_x^+ = \text{Var}[\mathbf{x}|\mathbf{m}_0^-, v_0^- \mathbf{1}]$
 $\bar{v}_x^+ = \text{mean}(\mathbf{v}_x^+)$
 $v_0^+ = 1 \odot (1 \odot \bar{v}_x^+ - 1 \odot v_0^-)$
 $\mathbf{m}_0^+ = (v_0^+ \mathbf{1}) \odot (\hat{\mathbf{x}}^+ \odot (v_0^+ \mathbf{1}) - \mathbf{m}_0^- \odot (v_0^- \mathbf{1}))$
 $\Psi^{-1} = \text{function_matrix_inverse}[\Psi(v_1^-, v_0^+)]$
 $\mathbf{Q}_x^+ = (\mathbf{F}_N \otimes \mathbf{I}_M) \Psi^{-1} (\mathbf{F}_N^H \otimes \mathbf{I}_M)$
 $\mathbf{m}_x^+ = \mathbf{Q}_x^+ (\mathbf{H}^H \text{Diag}(\mathbf{1} \odot (v_1^- \mathbf{1})) \mathbf{m}_1^- + \mathbf{m}_0^+ \odot (v_0^+ \mathbf{1}))$
 $\hat{\mathbf{z}}^+ = \mathbf{H} \mathbf{m}_x^+$
 $\mathbf{v}_z^+ = \text{diag}(\mathbf{H} \mathbf{Q}_x^+ \mathbf{H}^H)$
 $\bar{v}_z^+ = \text{mean}(\mathbf{v}_z^+)$
 $v_1^+ = 1 \odot (1 \odot \bar{v}_z^+ - 1 \odot v_1^-)$
 $\mathbf{m}_1^+ = (v_1^+ \mathbf{1}) \odot (\hat{\mathbf{z}}^+ \odot (v_1^+ \mathbf{1}) - \mathbf{m}_1^- \odot (v_1^- \mathbf{1}))$
 $t = t + 1$
end
Output: $\hat{\mathbf{x}}^+$

$$= \begin{bmatrix} \mathbf{U}^{-1} \mathbf{L}^{-1} + \mathbf{U}^{-1} \mathbf{E} (\mathbf{F} \mathbf{G})^{-1} \mathbf{V} \mathbf{L}^{-1} & -\mathbf{U}^{-1} \mathbf{E} (\mathbf{F} \mathbf{G})^{-1} \\ -(\mathbf{F} \mathbf{G})^{-1} \mathbf{V} \mathbf{L}^{-1} & (\mathbf{F} \mathbf{G})^{-1} \end{bmatrix} \triangleq \text{function_matrix_inverse}[\Psi] \quad (8)$$

So far, we have reduced the complexity of the most demanding operation of GEC-SR [12] from $\mathcal{O}((MN)^3)$ to $\mathcal{O}(l_{\max}^2 MN)$. Further replacing Eq. (13a) and (17a) of [12, Algorithm 1] with $\text{function_matrix_inverse}[\Psi]$ above, we finally obtain a new algorithm, whose computational efficiency is significantly higher. For the readers' convenience, we present this as Algorithm 1, where \odot and \oslash are component-wise product and division, respectively, and

$$\mathbb{E}[\mathbf{x}|\mathbf{m}, \mathbf{v}] = \frac{\int \mathbf{x} p(\mathbf{x}) \mathcal{N}(\mathbf{x}|\mathbf{m}, \mathbf{v}) d\mathbf{x}}{\int p(\mathbf{x}) \mathcal{N}(\mathbf{x}|\mathbf{m}, \mathbf{v}) d\mathbf{x}}$$

$$\text{Var}[\mathbf{x}|\mathbf{m}, \mathbf{v}] = \frac{\int |\mathbf{x} - \mathbb{E}[\mathbf{x}|\mathbf{m}, \mathbf{v}]|^2 p(\mathbf{x}) \mathcal{N}(\mathbf{x}|\mathbf{m}, \mathbf{v}) d\mathbf{x}}{\int p(\mathbf{x}) \mathcal{N}(\mathbf{x}|\mathbf{m}, \mathbf{v}) d\mathbf{x}}$$

with $\mathcal{N}(\cdot|\mathbf{m}, \mathbf{v})$ being Gaussian PDF of mean \mathbf{m} and covariance $\text{Diag}(\mathbf{v})$, while $\mathbb{E}[\mathbf{z}|\mathbf{m}, \mathbf{v}]$ and $\text{Var}[\mathbf{z}|\mathbf{m}, \mathbf{v}]$ are similarly defined, except $p(\mathbf{x})$ is replaced by $p(\mathbf{y}|\mathbf{z})$ and \mathbf{x} by \mathbf{z} .

The overall complexity of the proposed algorithm is then $\mathcal{O}(TMN(l_{\max}^2 + |\mathcal{A}|))$, where l_{\max} is the number of delay taps, T is the number of algorithm iterations, and $|\mathcal{A}|$ is the constellation size of a modulated symbol, e.g., $|\mathcal{A}| = 4$ for QPSK. Comparing with GEC-SR's complexity $\mathcal{O}(T(MN)^3)$ [12], our algorithm is far more efficient, because $(l_{\max}^2 + |\mathcal{A}|) \ll (MN)^2$, given that M and N are both large. Our complexity is also much lower than other matrix-inversion-based algorithms of complexity $\mathcal{O}((MN)^3)$, such as classical MMSE [27] and ML-VAMP [24], since, empirically, $T \approx 10$, $l_{\max} \approx 10$, and $T(l_{\max}^2 + |\mathcal{A}|) \ll (MN)^2$. Summing up,

TABLE I
COMPARISON OF COMPLEXITY

Algorithm	Complexity	Algorithm	Complexity
ML-VAMP[24]	$\mathcal{O}((MN)^3)$	GEC-SR[12]	$\mathcal{O}(T(MN)^3)$
LMMSE[27]	$\mathcal{O}((MN)^3)$	Proposed	$\mathcal{O}(TMN(l_{\max}^2 + \mathcal{A}))$

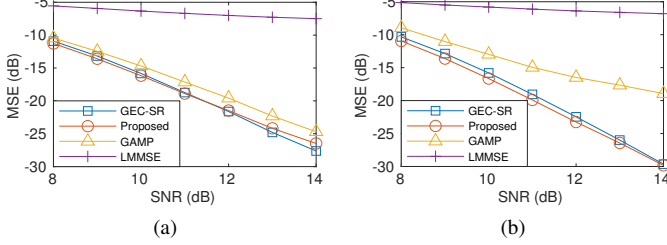


Fig. 4. The proposed algorithm is robust to the change of propagation path: (a) $P = 6$, (b) $P = 14$.

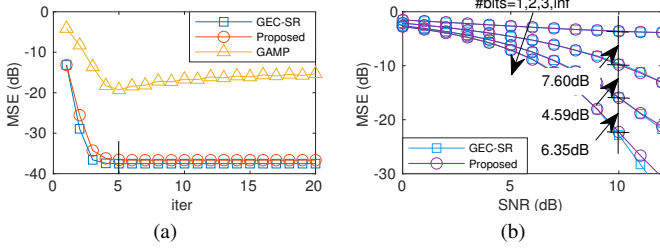


Fig. 5. The proposed algorithm performs equally good as the $\mathcal{O}((MN)^3)$ -complexity GEC-SR at only the cost of $\mathcal{O}(MN)$ multiplications per iteration: (a) $P = 14$, ∞ -bit, and SNR = 12 dB; (b) $P = 6$.

the proposed algorithm has the lowest complexity, as we summarize in Table I.

It is also worthy of noting although Eq. (6) here looks very similar to [8, Eq. (40)], the assumptions underlying these equations are very different: [8] relied on the assumption of an ideal quantization to derive a time-domain effective model [8, Eq. (39)]; in case of coarse quantization, [8, Eq. (39)] no longer holds, and the method there did not apply. By contrast, our method applies to a much broader scope, including coarse quantization as a special case.

IV. SIMULATION RESULTS

To validate the effectiveness of our algorithm, we consider the following setup: sub-carrier number $M = 32$, slot number $N = 8$, QPSK modulation, maximum delay taps $l_{\max} = 14$, maximum Doppler shift taps $k_{\max} = 6$. The delay index l_i is randomly drawn from the integer uniform distribution $U_i[1, l_{\max}]$, with the first tap fixed at $l_1 = 0$. The Doppler index k_i is also uniformly drawn but from $U_i[-k_{\max}, k_{\max}]$, while the channel gain h_i is Gaussian distributed as $\mathcal{N}(0, 1/P)$.

Fig. 4 compares the MSE performance of LMMSE, GAMP, GEC-SR and our algorithm over the entire SNR range by fixing the quantization at 3-bit. Clearly, we see that our algorithm outperforms GAMP [11] in both cases as the number of propagation paths P increases from 6 to 14. Meanwhile,

its performance is almost as good as GEC-SR [12], although our complexity is significantly lower (as discussed before).

Fig. 5a further studies the per-iteration behavior of the three, GAMP, GEC-SR, and the proposed, at 12 dB SNR. It is shown that our proposal converges very quickly: it hits the error floor within 5 iterations, which is as fast as GEC-SR. By contrast, GAMP fluctuates even after it hits the lowest point.

Fig. 5b showcases the impact of quantization precision on symbol detection. We decrease the number of quantization bits from infinite to 3, 2, and 1, and see that, interestingly, empowered by our algorithm, the loss of using a 3-bit coarse quantization is only 6.35 dB, as compared to the ideal case with infinite precision. It is worthy mentioning today's communication systems typically use a 8-bit ADC [1], which means there is still room for improvement in cost saving.

V. CONCLUSION

OTFS is a an enabler for future wireless communications that convey information in the delay-Doppler domain. For OTFS, this paper explicitly modeled a coarse and noisy quantization in the system. Our contributions are two-folded: firstly, we found that with coarse quantization, the effective channel was imbalanced and non-isotropic, which made it fail to circularly shift the transmitted symbols along the delay-Doppler domain, and also imposed a significant performance loss to the detection of symbols; secondly, we proposed a low-complexity detection algorithm that incorporates into GEC-SR a quick inversion for the quasi-banded matrices. Our proposal can reduce the complexity from a cubic order to a linear order, while keeping the performance at the same level.

APPENDIX

Consider a noisy quantization process

$$y = \mathbb{Q}[z + w], \quad (9)$$

where y is the quantization output, z is the input, and w is an AWGN with variance σ^2 . In case of B -bit uniform quantization with step size Δ , the mapping of $\mathbb{Q}[\cdot]$ can be expressed as: $\mathbb{Q}[z] = p_1 + \Delta \sum_{i=2}^{2^B} \mathcal{H}[z - q_i]$, where $p_1 = (-2^{B-1} + \frac{1}{2})\Delta$, and q_i is the lower limit of the i -th quantization interval, i.e., $q_1 = -\infty$, $q_2 = (1 - 2^{B-1})\Delta$, $q_{i+1} = q_i + \Delta$, ($i = 2, 3, \dots, 2^B - 1$), and $q_{2^B+1} = +\infty$. $\mathcal{H}[z]$ is a Heaviside function, i.e., it equals 1 if $z > 0$ and 0 otherwise. The transitional probability density from a complex z to a complex y is then given by

$$p(y|z) = f_{\text{out}}(\Re\{y\}|\Re\{z\}) f_{\text{out}}(\Im\{y\}|\Im\{z\})$$

where $f_{\text{out}}(\bar{y}|\bar{z}) = \sum_i \delta(\bar{y} - p_i) \left[\Phi\left(\frac{q_{i+1} - \bar{z}}{\sqrt{\sigma^2/2}}\right) - \Phi\left(\frac{q_i - \bar{z}}{\sqrt{\sigma^2/2}}\right) \right]$, $\Re\{\cdot\}$ and $\Im\{\cdot\}$ are the real and imaginary parts of a complex number, respectively, $\delta(x)$ is the Dirac delta function, $p_{i+1} = p_i + \Delta$ with $i = 1, 2, \dots, 2^B - 1$, and $\Phi(x) = \int_{-\infty}^x \mathcal{N}(t|0, 1) dt$.

REFERENCES

- [1] P. Stoica, X. Shang, and Y. Cheng, "The Cramér–Rao bound for signal parameter estimation from quantized data," *IEEE Signal Process. Mag.*, vol. 39, no. 1, pp. 118–125, 2021.
- [2] X. You, C.-X. Wang, J. Huang, X. Gao, Z. Zhang, M. Wang, Y. Huang, C. Zhang, Y. Jiang, J. Wang *et al.*, "Towards 6G wireless communication networks: Vision, enabling technologies, and new paradigm shifts," *Sci. China: Inf. Sci.*, vol. 64, pp. 1–74, 2021.
- [3] R. Hadani, S. Rakib, M. Tsatsanis, A. Monk, A. J. Goldsmith, A. F. Molisch, and R. Calderbank, "Orthogonal time frequency space modulation," in *IEEE WCNC*. IEEE, 2017, pp. 1–6.
- [4] S. S. Das and R. Prasad, *OTFS: Orthogonal Time Frequency Space Modulation A Waveform for 6G*. River Publishers, 2022.
- [5] S. Li, W. Yuan, Z. Wei, J. Yuan, B. Bai, D. W. K. Ng, and Y. Xie, "Hybrid map and pic detection for ofts modulation," *IEEE Trans. Veh. Technol.*, vol. 70, no. 7, pp. 7193–7198, 2021.
- [6] S. Li, W. Yuan, Z. Wei, and J. Yuan, "Cross domain iterative detection for orthogonal time frequency space modulation," *IEEE Trans. Wireless Commun.*, vol. 21, no. 4, pp. 2227–2242, 2021.
- [7] P. Raviteja, K. T. Phan, Y. Hong, and E. Viterbo, "Interference cancellation and iterative detection for orthogonal time frequency space modulation," *IEEE Trans. Wireless Commun.*, vol. 17, no. 10, pp. 6501–6515, 2018.
- [8] Y. Shan, F. Wang, and Y. Hao, "Orthogonal time frequency space detection via low-complexity expectation propagation," *IEEE Trans. Wireless Commun.*, vol. 21, no. 12, pp. 10887–10901, 2022.
- [9] Z. Yuan, F. Liu, W. Yuan, Q. Guo, Z. Wang, and J. Yuan, "Iterative detection for orthogonal time frequency space modulation with unitary approximate message passing," *IEEE Trans. Wireless Commun.*, vol. 21, no. 2, pp. 714–725, 2021.
- [10] N. Wu, Y. Zhang, Y. Ma, B. Li, and W. Yuan, "Vector approximate message passing based iterative receiver for ofts system," in *IEEE/CIC ICC Workshops*. IEEE, 2021, pp. 422–426.
- [11] S. Rangan, "Generalized approximate message passing for estimation with random linear mixing," in *IEEE Int. Symp. Inf. Theory - Proc.* IEEE, 2011, pp. 2168–2172.
- [12] H. He, C.-K. Wen, and S. Jin, "Generalized expectation consistent signal recovery for nonlinear measurements," in *IEEE ISIT*. IEEE, 2017, pp. 2333–2337.
- [13] S. Tiwari, S. S. Das, and V. Ranganmari, "Low complexity LMMSE receiver for OTFS," *IEEE Commun. Lett.*, vol. 23, no. 12, pp. 2205–2209, 2019.
- [14] P. Raviteja, Y. Hong, E. Viterbo, and E. Biglieri, "Practical pulse-shaping waveforms for reduced-cyclic-prefix OTFS," *IEEE Trans. Veh. Technol.*, vol. 68, no. 1, pp. 957–961, 2018.
- [15] P. Raviteja, K. T. Phan, Q. Jin, Y. Hong, and E. Viterbo, "Low-complexity iterative detection for Orthogonal Time Frequency Space modulation," in *IEEE WCNC*, 2018, pp. 1–6.
- [16] C.-K. Wen, S. Jin, K.-K. Wong, C.-J. Wang, and G. Wu, "Joint channel-and-data estimation for large-mimo systems with low-precision adcs," in *IEEE ISIT*. IEEE, 2015, pp. 1237–1241.
- [17] C.-K. Wen, C.-J. Wang, S. Jin, K.-K. Wong, and P. Ting, "Bayes-optimal joint channel-and-data estimation for massive MIMO with low-precision ADCs," *IEEE Trans. Signal Process.*, vol. 64, no. 10, pp. 2541–2556, 2015.
- [18] Q. Zou, H. Zhang, D. Cai, and H. Yang, "A low-complexity joint user activity, channel and data estimation for grant-free massive MIMO systems," *IEEE Signal Process. Lett.*, vol. 27, pp. 1290–1294, 2020.
- [19] —, "Message passing based joint channel and user activity estimation for uplink grant-free massive MIMO systems with low-precision ADCs," *IEEE Signal Process. Lett.*, vol. 27, pp. 506–510, 2020.
- [20] J. Mo, P. Schniter, N. G. Prelcic, and R. W. Heath, "Channel estimation in millimeter wave MIMO systems with one-bit quantization," in *48th Asilomar Conf. Signals Syst. Comput.* IEEE, 2014, pp. 957–961.
- [21] S. Liu, H. Zhang, and Q. Zou, "Decentralized channel estimation for the uplink of grant-free massive machine-type communications," *IEEE Trans. Commun.*, vol. 70, no. 2, pp. 967–979, 2021.
- [22] D. L. Donoho, A. Maleki, and A. Montanari, "Message-passing algorithms for compressed sensing," *Proc. Natl. Acad. Sci.*, vol. 106, no. 45, pp. 18 914–18 919, 2009.
- [23] T. P. Minka, "A family of algorithms for approximate bayesian inference," Ph.D. dissertation, Massachusetts Institute of Technology, 2001.
- [24] A. K. Fletcher, S. Rangan, and P. Schniter, "Inference in deep networks in high dimensions," in *IEEE ISIT*. IEEE, 2018, pp. 1884–1888.
- [25] *Wireless LAN Medium Access Control (MAC) and Physical Layer (PHY) Specification*, IEEE Std. 802.11, 1997.
- [26] D. W. Walker, T. Aldcroft, A. Cisneros, G. C. Fox, and W. Furmanski, "LU decomposition of banded matrices and the solution of linear systems on hypercubes," in *Proc. of the third Conf. on C3P*, vol. 2, 1989, pp. 1635–1655.
- [27] S. M. Kay, *Fundamentals of Statistical Signal Processing: Estimation Theory*. Pearson Education, 1993.